



Usefulness of Arterial Subtraction in Applying Liver Imaging Reporting and Data System (LI-RADS) Treatment Response Algorithm to Gadoteric Acid-Enhanced MRI

Seo Yeon Youn¹, Dong Hwan Kim¹, Joon-Il Choi^{1,2}, Moon Hyung Choi³, Bohyun Kim¹, Yu Ri Shin¹, Soon Nam Oh¹, Sung Eun Rha¹

¹Department of Radiology, Seoul St. Mary's Hospital, College of Medicine, The Catholic University of Korea, Seoul, Korea;

²Cancer Research Institute, College of Medicine, The Catholic University of Korea, Seoul, Korea;

³Department of Radiology, Eunpyeong St. Mary's Hospital, College of Medicine, The Catholic University of Korea, Seoul, Korea

Objective: We aimed to evaluate the usefulness of arterial subtraction images for predicting the viability of hepatocellular carcinoma (HCC) after locoregional therapy (LRT) using gadoteric acid-enhanced MRI and the Liver Imaging Reporting and Data System treatment response (LR-TR) algorithm.

Materials and Methods: This study included 90 patients (mean age \pm standard deviation, 57 ± 9 years) who underwent liver transplantation or resection after LRT and had 73 viable and 32 nonviable HCCs. All patients underwent gadoteric acid-enhanced MRI before surgery. Two radiologists assessed the presence of LR-TR features, including arterial phase hyperenhancement (APHE) and LR-TR categories (viable, nonviable, or equivocal), using ordinary arterial-phase and arterial subtraction images. The reference standard for tumor viability was surgical pathology. The sensitivity of APHE for diagnosing viable HCC was compared between ordinary arterial-phase and arterial subtraction images. The sensitivity and specificity of the LR-TR algorithm for diagnosing viable HCC was compared between the use of ordinary arterial-phase and the use of arterial subtraction images. Subgroup analysis was performed on lesions treated with transarterial chemoembolization (TACE) only.

Results: The sensitivity of APHE for viable HCCs was higher for arterial subtraction images than ordinary arterial-phase images (71.2% vs. 47.9%; $p < 0.001$). LR-TR viable category with the use of arterial subtraction images compared with ordinary arterial-phase images showed a significant increase in sensitivity (76.7% [56/73] vs. 63.0% [46/73]; $p = 0.002$) without significant decrease in specificity (90.6% [29/32] vs. 93.8% [30/32]; $p > 0.999$). In a subgroup of 63 lesions treated with TACE only, the use of arterial subtraction images showed a significant increase in sensitivity (81.4% [35/43] vs. 67.4% [29/43]; $p = 0.031$) without significant decrease in specificity (85.0% [17/20] vs. 90.0% [18/20]; $p > 0.999$).

Conclusion: Use of arterial subtraction images compared with ordinary arterial-phase images improved the sensitivity while maintaining specificity for diagnosing viable HCC after LRT using gadoteric acid-enhanced MRI and the LR-TR algorithm.

Keywords: Hepatocellular carcinoma; Magnetic resonance imaging; Gadoteric acid; Response assessment; Subtraction technique

INTRODUCTION

Hepatocellular carcinoma (HCC) is the fourth most frequent cause of cancer-related deaths, and its incidence has been rapidly increasing over the last two decades [1,2].

Several potentially curative or palliative treatments for HCC have been proposed for various cancer stages [3,4]. Among these treatments, the use of locoregional therapy (LRT), such as radiofrequency ablation (RFA) and transarterial chemoembolization (TACE), has been increasing, and LRT

Received: November 26, 2020 **Revised:** January 21, 2021 **Accepted:** February 16, 2021

Corresponding author: Dong Hwan Kim, MD, Department of Radiology, Seoul St. Mary's Hospital, College of Medicine, The Catholic University of Korea, 222 Banpo-daero, Seocho-gu, Seoul 06591, Korea.

• E-mail: kimdh@catholic.ac.kr

This is an Open Access article distributed under the terms of the Creative Commons Attribution Non-Commercial License (<https://creativecommons.org/licenses/by-nc/4.0>) which permits unrestricted non-commercial use, distribution, and reproduction in any medium, provided the original work is properly cited.

can be used with a curative intent as a definite treatment for early-stage HCC, a bridging procedure before liver transplantation (LT), or with a palliative intent to treat advanced disease [3-5]. Following LRT for HCC, the accurate assessment of treatment response is of great importance for determining treatment success, guiding future treatment strategies, and predicting patient prognosis [6,7].

To improve consistency and standardize the imaging criteria for HCC after LRT, the Liver Imaging Reporting and Data System (LI-RADS) introduced a new treatment response algorithm in 2017 [8]. Unlike several patient-level treatment response criteria, including modified Response Evaluation Criteria in Solid Tumors (mRECIST) and European Association for the Study of the Liver (EASL), which consider arterial phase hyperenhancement (APHE) as the only characteristic of a viable tumor [9,10], the LI-RADS treatment response (LR-TR) algorithm includes “washout” and “enhancement similar to pretreatment” as additional features of a viable tumor [8,11]. Although all three features were significantly associated with tumor viability, APHE was the most frequently observed feature of viable tumors (71.6–96.4%) and the most predictive of pathologic necrosis [12-15]. Therefore, it is of utmost importance to detect APHE during the treatment response evaluation of HCC.

HCCs treated with LRT present a bright appearance on precontrast T1-weighted images due to intratumoral necrosis, which may hamper the detection of APHE on MRI and lower the sensitivity for diagnosing viable tumors [16]. Furthermore, since arterial-phase enhancement on gadoxetic acid (Eovist/Primovist; Bayer HealthCare) is weaker than that of extracellular contrast agents, the detection rate of viable HCCs for gadoxetic acid-enhanced MRI may be lower than that for extracellular contrast-enhanced MRI [17]. Arterial subtraction images have been proposed to overcome these shortcomings and are helpful for accurately assessing treatment response and diagnosing HCC [18-20]. Recently, Gordic et al. [19] reported that MRI subtraction imaging has excellent diagnostic performance for predicting the pathological degree of HCC necrosis after LRT. However, the clinical utility of arterial subtraction gadoxetic acid-enhanced MRI in predicting the viability of HCC treated with LRT has not been investigated using the LR-TR algorithm.

The present study aimed to evaluate the usefulness of arterial subtraction images for predicting the viability of HCC treated with LRT using gadoxetic acid-enhanced MRI and the LR-TR algorithm.

MATERIALS AND METHODS

Study Population

Our Institutional Review Board approved this study, and the requirement for informed consent was waived because of its retrospective design (IRB No. KC20RASI0302). An institutional database search identified 585 consecutive patients who underwent LT or surgical resection for HCC between January 2011 and June 2016 (Fig. 1). Patients were included if they 1) underwent LT or resection for HCC, 2) underwent LRT for HCC before surgery, and 3) underwent post-treatment gadoxetic acid-enhanced MRI within 90 days before surgery. Among the 585 patients, 436 patients were excluded for not undergoing LRT (n = 392) or post-treatment gadoxetic acid-enhanced MRI within 90 days before surgery (n = 44). Of the remaining 149 patients who underwent LRT for HCC, 57 were excluded because they 1) had no dynamic liver CT or MRI before LRT (n = 45), 2) underwent combined systemic therapy (n = 4), 3) underwent subtotal resection for HCC (n = 2), or 4) had multiple HCCs which made a radiopathologic correlation between post-treatment MRI and a pathologic report not possible (n = 6). For the remaining 92 patients, one author analyzed the image quality of arterial subtraction images obtained with post-treatment MRI using a 5-point scale (Supplementary Material) [21] -grades 4 and 5 regarded as satisfactory image quality. As a result, two patients were excluded because of unsatisfactory image quality. A total of 90 patients with 105 HCCs were included in this study.

MRI Techniques

All patients underwent MRI examinations using a 3T (n = 88; Magnetom Verio, Siemens Healthcare) or 1.5T scanner (n = 2; Achieva, Philips Healthcare). Unenhanced MRI included T1-weighted dual gradient-echo in- and opposed-phase imaging, T2-weighted multi-shot and single-shot fast spin-echo imaging, and diffusion-weighted single-shot spin-echo echo-planar imaging. For contrast-enhanced dynamic imaging, 0.025 mmol/kg of gadoxetic acid was injected at a rate of 2.0 mL/s using an automated infusion system followed by a subsequent 20 mL saline flush. Three-dimensional gradient-recalled echo imaging was performed during the single arterial phase (30–35 seconds using a bolus-tracking technique), portal venous phase (65–80 seconds after contrast agent injection), transitional phase (3 minutes after contrast agent injection), and hepatobiliary phase (20 minutes after contrast agent

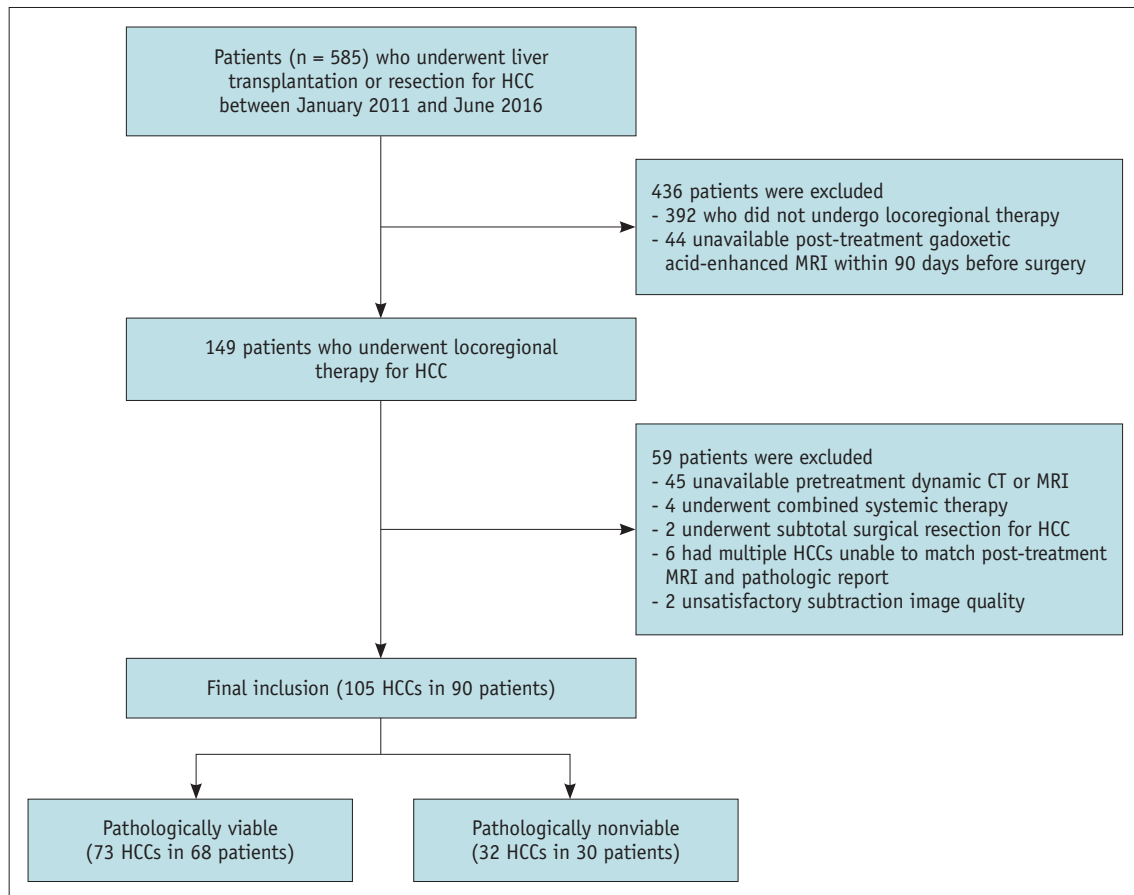


Fig. 1. Flow diagram for subject selection. HCC = hepatocellular carcinoma

injection). Subtraction images were automatically generated by a commercially available co-registration software that provided image-by-image subtraction between the unenhanced and arterial phases of each patient after the image acquisition. The detailed protocol for MRI acquisition is presented in Supplementary Table 1.

MR Image Analysis and LI-RADS Treatment Response Category Assignment

MR images were anonymized, randomized, and independently reviewed by two board-certified abdominal radiologists (with 6 and 9 years of experience in hepatic imaging, respectively). The reviewers were aware that all patients had undergone LRT for HCC and were allowed to review pretreatment CT or MRI. However, they were blinded to the clinical information of the individual patients, including the final pathological results and the evaluation outcomes of the other reviewer. Another radiologist (with 12 years of experience in hepatic imaging) analyzed the lesions on pretreatment CT or MRI and assigned a final LI-RADS category according to LI-RADS v2018 [22].

To evaluate HCC viability after LRT according to the LI-RADS [8], both reviewers assessed the presence of LR-TR features, including the following: 1) no lesional enhancement; 2) treatment-specific expected enhancement; 3) nodular, mass-like, or irregular thick tissue (NMLIT) within or along the treated lesion with APHE; 4) NMLIT with washout appearance; 5) NMLIT with enhancement similar to pretreatment imaging. If lesional enhancement could not be evaluated due to image degradation or omission, the lesion was considered as LR-TR non-evaluable. Treated lesions showing NMLIT with APHE, washout appearance, or enhancement similar to pretreatment were considered LR-TR viable. The LR-TR nonviable category was assigned to lesions with treatment-specific expected enhancement or no lesional enhancement. If enhancement was atypical for the treatment-specific expected enhancement pattern and did not meet the criteria for LR-TR viable or nonviable, the lesion was considered LR-TR equivocal. Each reviewer measured the size of the LR-TR viable or equivocal lesions and assessed the signal intensity (hyperintense, isointense, hypointense) of the treated lesions on precontrast T1-

weighted images.

For the image interpretation as mentioned above, the reviewers evaluated the presence of APHE in two separate sessions, first using ordinary arterial-phase images and subsequently using arterial subtraction images, with a 4-week interval to minimize recall bias. Discrepancies between the two reviewers in the interpretation of LR-TR features and the final LR-TR category were resolved at a consensus meeting in the presence of a third reviewer. The consensus results were used for study analysis.

Reference Standard

The reference standards for HCC viability were based on surgical pathology. To achieve precise radiologic-pathologic correlation, one of the authors who did not participate in the image review ensured concordance between post-treatment MRI and pathologic reports for all included lesions. All included lesions were accurately described in the pathologic reports, including location, size, viability, and/or percentage of necrosis. The final pathologic diagnosis at our institution was mainly made by three pathologists with more than 5 years of experience in liver pathology. Non-necrotic or partially necrotic HCC was considered a pathologically viable lesion. Totally necrotic HCC (percentage of necrosis, 100%) was considered a pathologically nonviable lesion.

Statistical Analysis

The LR-TR features, NMLIT with APHE on arterial subtraction images, and final LR-TR category were compared between pathologically viable and nonviable groups using chi-squared or Fisher's exact tests for categorical variables, and Mann-Whitney U or Student's *t* tests for continuous variables.

The sensitivity of APHE for detecting pathologically viable HCC was compared between ordinary arterial-phase images and arterial subtraction images using McNemar's test. To assess the usefulness of arterial subtraction images in predicting HCC viability using the LR-TR algorithm, the sensitivities and specificities of 'LR-TR viable' and 'LR-TR viable or equivocal' for diagnosing pathologically viable HCC were compared between the use of ordinary arterial-phase images and the use of arterial subtraction images using McNemar's test. Subgroup analyses were performed on the lesions treated with TACE only and according to precontrast T1-weighted signal intensity on post-treatment MRI.

Interobserver agreements for LR-TR features, NMLIT with

APHE on arterial subtraction images, and LR-TR categories were evaluated using the overall percentage of agreement and κ statistics. The agreement in the sizes of the viable or equivocally viable lesions were evaluated using the intraclass correlation coefficient (ICC).

Statistical significance was set at $p < 0.05$. Statistical analyses were performed using the SPSS software, version 24 (IBM Corp.).

RESULTS

Patient Characteristics

Among the 90 patients, 55 (61.1%) underwent LT and 35 (38.9%) underwent liver resection. There were 69 male (76.7%) and 21 female (23.3%) with a mean age of 57 years (range, 38–84 years). Hepatitis B disease ($n = 67$, 74.4%) was the predominant cause of chronic liver disease. Most lesions were classified as LI-RADS 5 ($n = 82$, 78.0%) on pretreatment CT or MRI, followed by LI-RADS 4 ($n = 15$, 14.3%). The most common type of LRT was TACE ($n = 60$, 57.0%). The second most common type was RFA ($n = 25$, 23.8%), followed by combined treatment with TACE and RFA ($n = 13$, 12.4%) and other treatments including drug-eluting bead (DEB)-TACE, transarterial radioembolization, percutaneous ethanol ablation, and combined treatment with DEB-TACE and RFA. The mean interval between LRT and post-treatment MRI was 269 days. There were 73 pathologically viable HCCs and 32 pathologically nonviable lesions in 90 patients. Of the 90 patients, 76 (84.4%) had a single lesion, 13 (14.4%) had two lesions, and one patient (1.1%) had three lesions. The clinical, radiologic, and pathologic characteristics of the 105 HCCs in 90 patients are summarized in Table 1.

Comparison of LR-TR Features and Category according to Tumor Viability

Arterial subtraction images detected NMLIT with APHE for pathologically viable lesions with a higher sensitivity than ordinary arterial-phase images (71.2% vs. 47.9%; $p < 0.001$) (Table 2). The detection rates of NMLIT with APHE on ordinary arterial-phase images, NMLIT with APHE on arterial subtraction images, NMLIT with washout appearance, and NMLIT with enhancement similar to pretreatment were significantly higher in the pathologically viable group than in the pathologically nonviable group ($p \leq 0.001$). Conversely, the detection rate of treatment-specific expected enhancement in the pathologically viable group

Table 1. Clinical-Pathologic and Radiologic Characteristics of 90 Patients

Characteristics	Total (n = 90)
Mean age, years (range)	57 (38–84)
Sex, male:female	69:21
No. of treated HCCs per patient	
1	76 (84.4)
2	13 (14.4)
3	1 (1.2)
Risk factors	
Hepatitis B	67 (74.4)
Hepatitis C	8 (8.9)
Alcoholic liver disease	6 (6.7)
Hepatitis B and alcoholic liver disease	4 (4.4)
Hepatitis C and alcoholic liver disease	1 (1.1)
Cryptogenic liver cirrhosis	4 (4.4)
Child-Pugh classification	
A	82 (91.1)
B	8 (8.9)
Median serum AFP (range), ng/mL	16.9 (1.6–30741.3)
Pretreatment LI-RADS category*	
LI-RADS 4	15 (14.3)
LI-RADS 5	82 (78.0)
LI-RADS M	1 (1.0)
LI-RADS TIV	7 (6.7)
Type of locoregional treatment*	
Conventional TACE	60 (57.0)
RFA	25 (23.8)
TACE + RFA	13 (12.4)
DEB - TACE	3 (2.9)
TARE	2 (1.9)
PEA	1 (1.0)
DEB - TACE + RFA	1 (1.0)
Type of surgery	
Surgical resection	35 (38.9)
Living donor liver transplantation	50 (55.6)
Deceased donor liver transplantation	5 (5.6)
Histopathologic necrosis, % [†]	
0	1 (1.0)
1–50	26 (26.3)
51–99	40 (40.4)
100% (pathologically nonviable)	32 (32.3)
Signal intensity on precontrast T1-WI*	
Iso- or hypointensity	65 (61.9)
Hyperintensity	40 (38.1)

Data are number (%) of patients unless specified otherwise. *Data are number (%) of lesions out of a total number of 105 lesions, [†]Six lesions were pathologically confirmed as viable HCC, but degree of necrosis was not reported in pathologic report. AFP = alpha-fetoprotein, DEB = drug-eluting beads, HCC = hepatocellular carcinoma, LI-RADS = Liver Imaging Reporting and Data System, PEA = percutaneous ethanol ablation, RFA = radiofrequency ablation, TACE = transarterial chemoembolization, TARE = transarterial radioembolization, TIV = tumor-in-vein, T1-WI = T1-weighted imaging

was significantly lower than that in the pathologically nonviable group (8.2% [6/73] vs. 37.5% [12/32]; $p < 0.001$).

The distributions of the final LR-TR categories between the pathologically viable and nonviable groups differed significantly ($p < 0.001$). Lesions in the pathologically viable group were more frequently classified as LR-TR viable (61.6% [45/73]), whereas those in the pathologically nonviable group were more frequently classified as LR-TR nonviable (87.5% [28/32]). Five lesions (6.8%) in the pathologically viable group and two lesions (6.3%) in the pathologically nonviable group were classified as LR-TR equivocal. No lesions were classified as LR-TR non-evaluable.

Diagnostic Performance of LR-TR Algorithm for Predicting Viable HCC

When LR-TR viable was considered as viable HCC, ordinary arterial-phase images showed a sensitivity of 63.0% (46/73) and a specificity of 93.8% (30/32) for the diagnosis of viable HCC (Table 3). When APHE was determined on arterial subtraction images, the sensitivity significantly increased to 76.7% (56/73; $p = 0.002$) with a comparable specificity of 90.6% (29/32; $p > 0.999$). Compared with ordinary arterial-phase images, the arterial subtraction images detected 10 additional viable HCCs at the cost of only one additional false-positive diagnosis (Figs. 2, 3). When both LR-TR viable and equivocal were diagnosed as viable HCC, the sensitivity of arterial subtraction images significantly increased to 83.6% (61/73) from 69.9% (51/73) ($p = 0.006$). The specificity decreased from 87.5% (28/32) to 75.0% (24/32), but this decrease was not statistically significant ($p = 0.125$) (Table 3).

Subgroup Analysis

In the subgroup analysis of 63 lesions treated with TACE only (Table 3), the sensitivity of LR-TR viable significantly improved when using arterial subtraction images (67.4% [29/43] vs. 81.4% [35/43], $p = 0.031$), whereas the specificity showed a slight decrease (90.0% [18/20] vs. 85.0% [17/20], $p > 0.999$). When both LR-TR viable and equivocal were considered as viable HCC, the differences in sensitivity and specificity between ordinary arterial-phase and arterial subtraction images were not statistically significant ($p = 0.219$ and $p = 0.250$, respectively).

An additional subgroup analysis was performed based on the precontrast T1-weighted signal intensity of the

Table 2. Prevalence of LR-TR Features on Gadoteric-Acid Enhanced MRI

	Pathologically Viable (n = 73)	Pathologically Nonviable (n = 32)	P
No lesional enhancement	13 (17.8)	11 (34.4)	0.063
Treatment-specific expected enhancement	6 (8.2)	12 (37.5)	< 0.001
NMLIT with APHE on ordinary arterial-phase images	35 (47.9)*	1 (3.1)	< 0.001
NMLIT with APHE on arterial subtraction images	52 (71.2)*	2 (6.3)	< 0.001
NMLIT with washout appearance	34 (46.6)	1 (3.1)	< 0.001
NMLIT with enhancement similar to pretreatment	23 (31.5)	1 (0.3)	0.001
Final LR-TR category			< 0.001
LR-TR viable	45 (61.6)	2 (6.3)	
LR-TR nonviable	23 (31.5)	28 (87.4)	
LR-TR equivocal	5 (6.9)	2 (6.3)	
Size of viable or equivocally viable disease, mm [†]	19.4 ± 11.0	15.5 ± 7.9	0.101

Unless otherwise indicated, data are number (%) of lesions. * $p < 0.001$ for comparing sensitivities between ordinary arterial-phase and arterial subtraction images, [†]Data are mean ± standard deviation. APHE = arterial phase hyperenhancement, LR-TR = Liver Imaging Reporting and Data System treatment response, NMLIT = nodular, mass-like, or irregular thick tissue in or along the treated lesion

Table 3. Comparison of Diagnostic Performance of LR-TR in Ordinary Arterial-Phase and Arterial Subtraction Images for Predicting Viable HCC

	Sensitivity (%)	P	Specificity (%)	P	Accuracy (%)
Total					
LR-TR viable		0.002*		> 0.999 [†]	
Ordinary arterial-phase images	63.0 (50.9–74.0) [46/73]		93.8 (79.2–99.2) [30/32]		72.4 (62.8–80.7) [76/105]
Arterial subtraction images	76.7 (65.4–85.8) [56/73]		90.6 (75.0–98.0) [29/32]		81.0 (72.1–88.0) [85/105]
LR-TR viable + equivocal		0.006 [‡]		0.125 [§]	
Ordinary arterial-phase images	69.9 (58.0–80.1) [51/73]		87.5 (71.0–96.5) [28/32]		75.2 (65.9–83.1) [79/105]
Arterial subtraction images	83.6 (73.4–94.9) [61/73]		75.0 (56.6–88.5) [24/32]		81.0 (72.1–88.0) [85/105]
TACE					
LR-TR viable		0.031*		> 0.999 [†]	
Ordinary arterial-phase images	67.4 (51.5–80.9) [29/43]		90.0 (68.3–98.8) [18/20]		74.6 (62.1–84.7) [47/63]
Arterial subtraction images	81.4 (66.6–91.6) [35/43]		85.0 (62.1–96.8) [17/20]		82.5 (70.9–91.0) [52/63]
LR-TR viable + equivocal		0.219 [‡]		0.250 [§]	
Ordinary arterial-phase images	79.1 (64.0–90.0) [34/43]		85.0 (62.1–96.8) [17/20]		81.0 (69.1–89.8) [51/63]
Arterial subtraction images	88.4 (74.9–96.1) [38/43]		70.0 (45.7–88.1) [14/20]		82.5 (70.9–91.0) [52/63]

Data in parentheses are 95% confidence intervals, and data in brackets are number of lesions. *Comparison of sensitivity between ordinary arterial-phase image and arterial subtraction image when LR-TR viable was regarded as viable HCC, [†]Comparison of specificity between ordinary arterial-phase image and arterial subtraction image when LR-TR viable was regarded as viable HCC, [‡]Comparison of sensitivity between ordinary arterial-phase image and arterial subtraction image when both LR-TR viable and equivocal were regarded as viable HCC, [§]Comparison of specificity between ordinary arterial-phase image and arterial subtraction image when both LR-TR viable and equivocal were regarded as viable HCC. HCC = hepatocellular carcinoma, LR-TR = Liver Imaging Reporting and Data System treatment response, TACE = transarterial chemoembolization

treated lesions on post-treatment MRI (Supplementary Table 2). For the 40 lesions showing T1 hyperintensity, the sensitivity of LR-TR viable increased from 34.8% (8/23) to 56.5% (13/23), and the specificity slightly decreased from 100% (17/17) to 94.1% (16/17) when arterial subtraction images were added. For the 65 lesions that showed T1 iso- or hypointensity, the sensitivity of LR-TR viable increased from 76.0% (38/50) to 86.0% (43/50), and the specificity remained the same at 86.7% (13/15) with the addition of

arterial subtraction images.

Discordant APHE between Ordinary Arterial-Phase and Arterial Subtraction Images

For the detection of NMLIT with APHE on ordinary arterial-phase and arterial subtraction images, 19 lesions (18.1%) showed a discrepancy between the two images; they did not manifest as APHE on arterial subtraction images but not on ordinary arterial-phase images. Of the 19

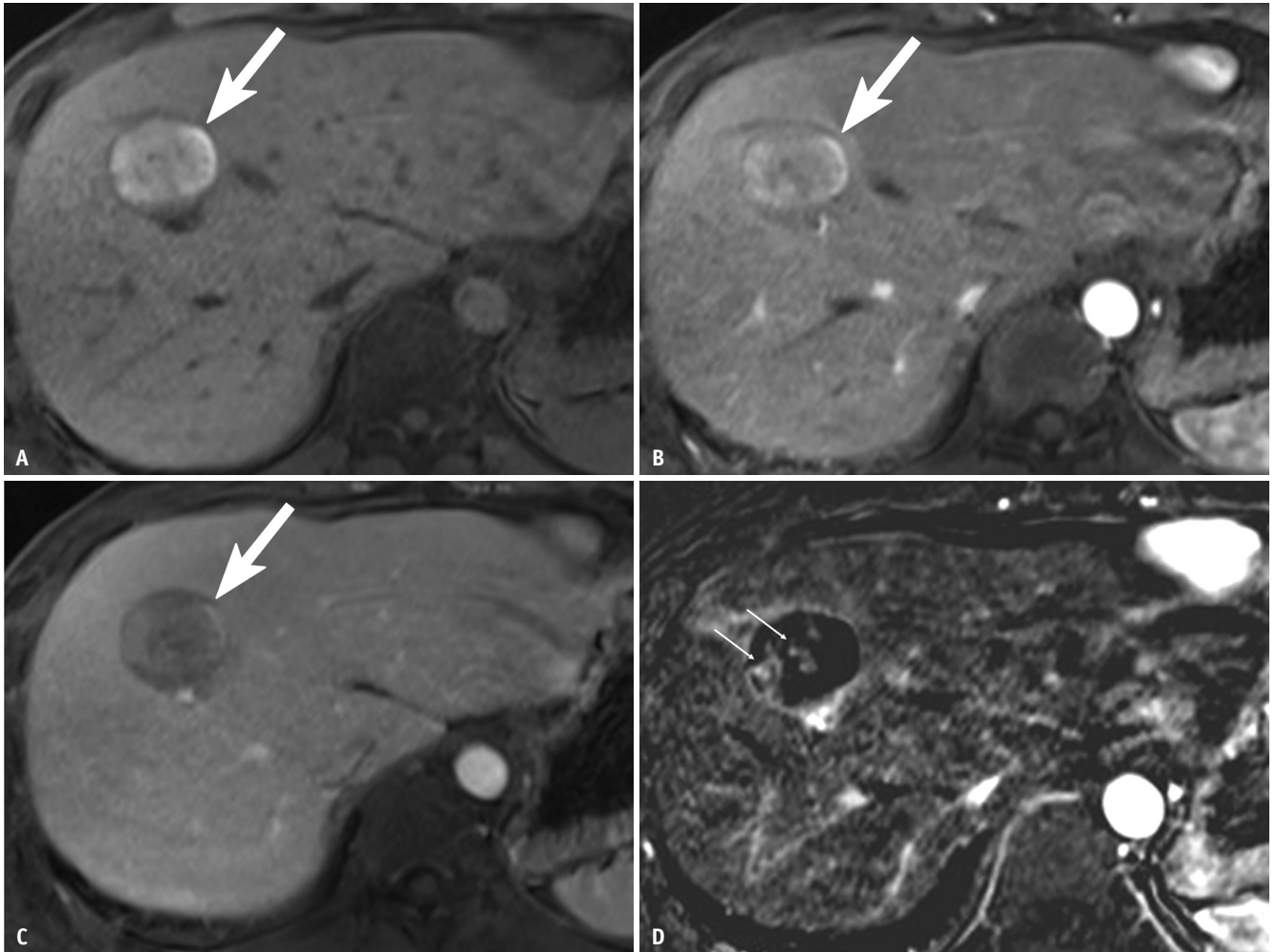


Fig. 2. HCC treated with TACE in a 38-year-old male with chronic hepatitis B.

A. Post-TACE precontrast T1-weighted MR image shows a 3.1 cm hyperintense lesion (arrow) in hepatic segment VIII. **B-D.** Ordinary arterial-phase image of gadoxetate acid-enhanced MRI does not depict APHE (**B**), and portal venous phase image does not show washout of the lesion (arrows) (**C**). However, (**D**) arterial subtraction image shows less than 1 cm of nodular tissue areas with APHE (arrows) within the treated lesion. The treated lesion was categorized as LR-TR nonviable based on ordinary arterial-phase images, and this category was changed to LR-TR viable when arterial subtraction images were used. Surgical pathology confirmed this lesion as viable HCC with 70% necrosis and background hemorrhagic necrosis. APHE = arterial phase hyperenhancement, HCC = hepatocellular carcinoma, LR-TR = Liver Imaging Reporting and Data System treatment response, TACE = transcatheter arterial chemoembolization

lesions, 18 lesions (94.7%) were confirmed as pathologically viable, and one lesion (5.3%) was confirmed as nonviable. The characteristics of the discordant lesions are summarized in Table 4.

Interobserver Agreement between Two Reviewers

The interobserver agreement for the LR-TR categorization on arterial subtraction images (overall percentage of agreement, 81.0%; κ , 0.661) was slightly higher than that for ordinary arterial-phase images (overall percentage of agreement, 77.1%; κ , 0.597) (Supplementary Table 3). The interobserver agreement was good for NMLIT with APHE on both ordinary arterial-phase images (κ = 0.750) and arterial

subtraction images (κ = 0.790). The agreement was also good for NMLIT with enhancement similar to pretreatment imaging (κ = 0.722). For all other LR-TR features, there were moderate interobserver agreements (κ = 0.469–0.524). The agreement for the size of the LR-TR viable or equivocal lesion was excellent (ICC, 0.842).

DISCUSSION

This study found that arterial subtraction images were more sensitive for detecting APHE for pathologically viable HCC treated with LRT than ordinary arterial-phase images (p < 0.001). The sensitivity of arterial subtraction gadoxetic

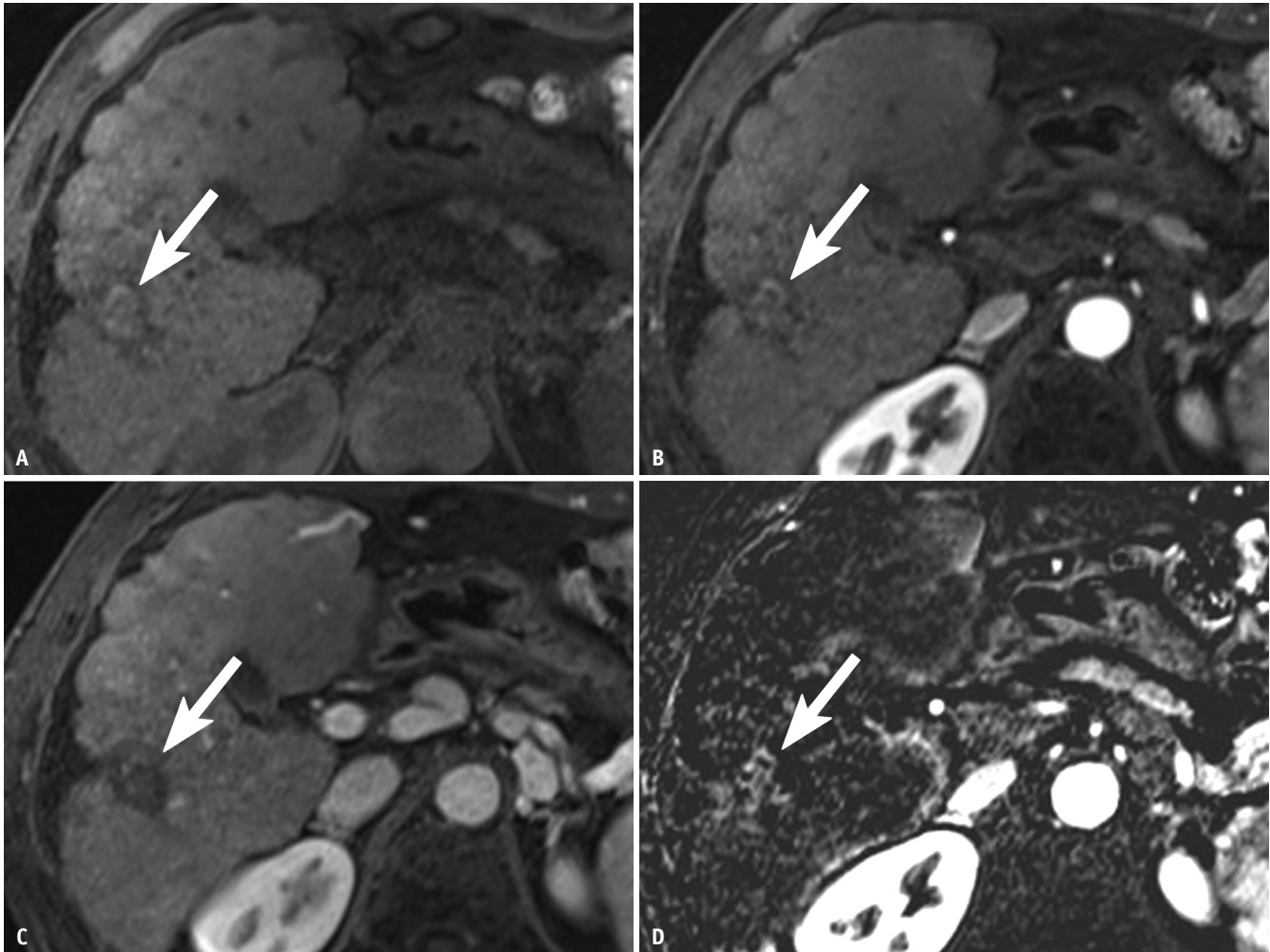


Fig. 3. HCC treated with a combination of transcatheter arterial chemoembolization and radiofrequency ablation in a 61-year-old male with cirrhosis due to chronic hepatitis B.

A. Post-treatment precontrast T1-weighted MR image shows a 2.5-cm hyperintense lesion (arrow) in hepatic segment VI. **B-D.** Ordinary arterial-phase image of gadoxetate acid-enhanced MRI does not depict arterial phase hyperenhancement (**B**), and portal venous phase image does not show washout of the lesion (arrows) (**C**). However, (**D**) arterial subtraction image shows hyperenhancement of 2.2-cm nodular enhancing area (arrow) along the posterolateral margin of the treated lesion. Therefore, the treated lesion was categorized as LR-TR nonviable based on ordinary arterial-phase images, whereas this category was changed to LR-TR viable when arterial subtraction images were used. Surgical pathology confirmed this lesion as nonviable HCC with 100% necrosis. This was a false-positive case based on the arterial subtraction images. HCC = hepatocellular carcinoma, LR-TR = Liver Imaging Reporting and Data System treatment response

acid-enhanced MRI for diagnosing viable HCC significantly increased (76.7% vs. 63.0%, $p = 0.002$) without a significant decrease in the specificity (90.6% vs. 93.8%, $p > 0.999$). In the subgroup analysis of lesions treated with TACE only, the sensitivity of the arterial subtraction images significantly increased to 81.4% from 67.4% for ordinary arterial-phase images ($p = 0.031$), with a minimal decrease in specificity to 85.0% from 90.0% ($p > 0.999$). The arterial subtraction images were also associated with a higher interobserver agreement than ordinary arterial-phase images for LR-TR categorization.

APHE is the most frequently observed imaging feature

(71.6–96.4%) among the three findings of the LR-TR viable criterion, which include APHE, washout, and enhancement similar to pretreatment imaging [13,14]. In addition, Shropshire et al. [12] demonstrated that the absence of APHE was associated with the highest area under the receiver operating characteristic curve (0.66–0.75) for predicting complete necrosis following LRT. Therefore, APHE is the most important imaging feature for diagnosing viability among the three findings of LR-TR viable. We found that the use of arterial subtraction images significantly improved the detection rate of APHE to 71.2% from 47.9% for pathologically viable lesions ($p < 0.001$). The use of

Table 4. Characteristics of 19 Lesions with Discordant APHE* between Ordinary Arterial-Phase Images and Arterial Subtraction Images

Characteristics	Total (n = 19)
Signal intensity on precontrast T1-weighted images	
Iso- or hypointensity	8 (42.1)
Hyperintensity	11 (57.9)
Pretreatment LI-RADS category	
LI-RADS 4	4 (21.1)
LI-RADS 5	14 (73.6)
LI-RADS TIV	1 (5.3)
Pathological viability	
Viable	18 (94.7)
Nonviable	1 (5.3)
Grade of viable HCC	
Edmondson-Steiner grade 2	11 (63.1)
Edmondson-Steiner grade 3	6 (31.6)
Edmondson-Steiner grade 4	1 (5.3)
Mean size, mm (range)	14.5 (5–49)
< 10	5 (26.3)
10–20	10 (52.5)
> 20	4 (21.2)
Change of LR-TR category [†]	
LR-TR nonviable to viable	9 (47.4)
LR-TR equivocal to viable	2 (10.5)
Not changed	8 (42.1)

Data are number (%) of lesions unless specified otherwise.

*Lesions not seen as APHE on ordinary arterial phase images but seen as APHE on arterial subtraction images, [†]Change in LR-TR category when arterial subtraction images were used. APHE = arterial phase hyperenhancement, HCC = hepatocellular carcinoma, LI-RADS = Liver Imaging Reporting and Data System, LR-TR = LI-RADS treatment response, TIV = tumor-in-vein

arterial subtraction images was more beneficial especially for treated lesions with precontrast T1 hyperintense or hemorrhagic necrosis after LRT. The sensitivity of LR-TR viable criterion with ordinary arterial-phase images for precontrast T1 hyperintense lesions was remarkably low at 34.8%, but it increased to 56.5% with the use of arterial subtracted images although the difference was not statistically significant ($p = 0.063$). The percentage of treated lesions with precontrast T1 hyperintensity was 57.9% (11/19) among the lesions with discordant APHE, whereas it was relatively low (38.1%, 40/105) in the entire study group. Despite its effect being relatively less pronounced, arterial subtraction images were also useful for T1 iso- or hypointense lesions; the sensitivity of LR-TR viable criterion increased from 76.0% to 86.0%. Given that weak arterial enhancement is a potential drawback of gadoteric acid-enhanced MRI [17], arterial subtraction

images can be clinically useful for the detection of APHE of treated lesions.

According to previous studies using MRI, the sensitivities of the LR-TR viable category were suboptimal, ranging from 30.4% to 75.9%, while the specificities ranged from 80.6% to 98.5% [13-15,23]. These results are similar to the sensitivity (63.0% [95% confidence interval (CI), 50.9–74.0%]) and specificity (93.8% [95% CI, 79.2–99.2%]) reported by the present study for ordinary arterial-phase images only. However, the use of arterial subtraction images resulted in higher sensitivity than ordinary arterial-phase images (76.7% vs. 63.0%, $p = 0.002$) without a significant loss of specificity (90.6% vs. 93.8%, $p > 0.999$). The arterial subtraction images detected 10 additional viable HCCs at the expense of only one additional false-positive diagnosis. For the false-positive case, a misregistration artifact associated with T1 hyperintensity of hemorrhagic necrosis within the treated lesion was mistaken for APHE. Although we only included lesions with grade 4 or 5 satisfactory image quality for arterial subtraction images, minute misregistration between the unenhanced and arterial phases may still exist; in rare cases, this may produce false-positive results. A limited number of studies have assessed the role of subtraction imaging in HCC after LRT [18,19,24]. Gordic et al. [19] reported excellent diagnostic performance of arterial subtraction imaging for predicting complete pathologic necrosis based on the mRECIST or EASL criteria (sensitivity, 86.9%; specificity, 73.9%). For LI-RADS v2018, arterial subtraction imaging was proposed as a technical recommendation [22], and our study is the first to demonstrate the usefulness of arterial subtraction images with the LR-TR algorithm.

Our results showed that two of the seven LR-TR equivocal lesions on ordinary arterial-phase images were classified as LR-TR viable based on arterial subtraction images, which resulted in additional true positive cases. On the contrary, one lesion was classified as LR-TR nonviable based on the arterial subtraction images, which resulted in an additional false-negative case. Therefore, we did not find a significant addition of value with the use of arterial subtraction images for the LR-TR equivocal category only. Given the few lesions classified as LR-TR equivocal in this study, further studies including a larger number of lesions are needed to validate this conjecture.

This study has several limitations. First, the inclusion of lesions pathologically confirmed through surgery may have introduced a selection bias. However, this allowed

the establishment of an ideal standard reference and quantitative evaluation of tumor necrosis after LRT. Second, the inclusion of various types of LRTs in the analysis may have caused heterogeneity, given that the degree of intratumoral hemorrhage and the expected post-treatment findings, which may have influenced the results, can vary depending on the type of LRT. We were unable to assess the performance of the LR-TR algorithm according to the LRT type due to the few patients involved, although subgroup analysis was performed for patients treated with TACE only to minimize this limitation. Third, a small proportion (2.2%, 2/92) of the included patients showed misregistration artifacts on arterial subtraction images, resulting in unsatisfactory image quality. This proportion was similar to that reported in previous studies (2.6–3%) [20,25]. In real practice, however, ordinary arterial-phase images can be used for cases with unsatisfactory quality of arterial subtraction images. Fourth, because of the relatively small number of pathologically nonviable lesions, the assessment of the specificity of the LR-TR algorithm may have been statistically underpowered.

In conclusion, arterial subtraction images can enhance the detection of APHE of viable HCC after LRT on gadoxetic acid-enhanced MRI. When applying the LR-TR algorithm, arterial subtraction images compared with ordinary arterial-phase images can significantly improve the sensitivity for predicting the viability of HCC while maintaining specificity.

Supplement

The Supplement is available with this article at <https://doi.org/10.3348/kjr.2020.1394>.

Conflicts of Interest

The authors have no potential conflicts of interest to disclose.

Author Contributions

Conceptualization: Dong Hwan Kim, Joon-Il Choi. Data curation: Seo Yeon Youn, Dong Hwan Kim, Moon Hyung Choi. Formal analysis: Seo Yeon Youn, Dong Hwan Kim, Joon-Il Choi, Bohyun Kim. Investigation: Seo Yeon Youn, Dong Hwan Kim, Joon-Il Choi, Bohyun Kim. Methodology: Seo Yeon Youn, Dong Hwan Kim. Project administration: Dong Hwan Kim. Resources: Seo Yeon Youn, Dong Hwan Kim. Supervision: Dong Hwan Kim. Visualization: Seo Yeon Youn, Dong Hwan Kim, Soon Nam Oh. Writing—original draft: Seo

Yeon Youn, Dong Hwan Kim. Writing—review & editing: Joon-Il Choi, Yu Ri Shin, Soon Nam Oh, Sung Eun Rha.

ORCID iDs

Seo Yeon Youn

<https://orcid.org/0000-0002-7692-3413>

Dong Hwan Kim

<https://orcid.org/0000-0002-2932-2367>

Joon-Il Choi

<https://orcid.org/0000-0003-0018-8712>

Moon Hyung Choi

<https://orcid.org/0000-0001-5962-4772>

Bohyun Kim

<https://orcid.org/0000-0003-1157-415X>

Yu Ri Shin

<https://orcid.org/0000-0001-5695-4426>

Soon Nam Oh

<https://orcid.org/0000-0003-2373-7024>

Sung Eun Rha

<https://orcid.org/0000-0003-1514-929X>

REFERENCES

1. El-Serag HB. Hepatocellular carcinoma. *N Engl J Med* 2011;365:1118-1127
2. Global Burden of Disease Liver Cancer Collaboration; Akinyemiju T, Abera S, Ahmed M, Alam N, Alemayohu MA, Allen C, et al. The burden of primary liver cancer and underlying etiologies from 1990 to 2015 at the global, regional, and national level: results from the global burden of disease study 2015. *JAMA Oncol* 2017;3:1683-1691
3. Bruix J, Sherman M; American Association for the Study of Liver Diseases. Management of hepatocellular carcinoma: an update. *Hepatology* 2011;53:1020-1022
4. Heimbach JK, Kulik LM, Finn RS, Sirlin CB, Abecassis MM, Roberts LR, et al. AASLD guidelines for the treatment of hepatocellular carcinoma. *Hepatology* 2018;67:358-380
5. Cescon M, Cucchetti A, Ravaioli M, Pinna AD. Hepatocellular carcinoma locoregional therapies for patients in the waiting list. Impact on transplantability and recurrence rate. *J Hepatol* 2013;58:609-618
6. Ho MH, Yu CY, Chung KP, Chen TW, Chu HC, Lin CK, et al. Locoregional therapy-induced tumor necrosis as a predictor of recurrence after liver transplant in patients with hepatocellular carcinoma. *Ann Surg Oncol* 2011;18:3632-3639
7. Allard MA, Sebahg M, Ruiz A, Guettier C, Paule B, Vibert E, et al. Does pathological response after transarterial chemoembolization for hepatocellular carcinoma in cirrhotic patients with cirrhosis predict outcome after liver resection or transplantation? *J Hepatol* 2015;63:83-92

8. American College of Radiology. CT/MRI LI-RADS® v2017. Acr.org Web site. <https://www.acr.org/Clinical-Resources/Reporting-and-Data-Systems/LI-RADS/CT-MRI-LI-RADS-v2017>. Accessed November 3, 2020
9. Lencioni R, Llovet JM. Modified RECIST (mRECIST) assessment for hepatocellular carcinoma. *Semin Liver Dis* 2010;30:52-60
10. Bruix J, Sherman M, Llovet JM, Beaugrand M, Lencioni R, Burroughs AK, et al. Clinical management of hepatocellular carcinoma. Conclusions of the Barcelona-2000 EASL conference. European Association for the Study of the Liver. *J Hepatol* 2001;35:421-430
11. Kiehl A, Fowler KJ, Lewis S, Yaghmai V, Miller FH, Yarmohammadi H, et al. Locoregional therapies for hepatocellular carcinoma and the new LI-RADS treatment response algorithm. *Abdom Radiol (NY)* 2018;43:218-230
12. Shropshire EL, Chaudhry M, Miller CM, Allen BC, Bozdogan E, Cardona DM, et al. LI-RADS treatment response algorithm: performance and diagnostic accuracy. *Radiology* 2019;292:226-234
13. Kim SW, Joo I, Kim HC, Ahn SJ, Kang HJ, Jeon SK, et al. LI-RADS treatment response categorization on gadoxetic acid-enhanced MRI: diagnostic performance compared to mRECIST and added value of ancillary features. *Eur Radiol* 2020;30:2861-2870
14. Seo N, Kim MS, Park MS, Choi JY, Do RKG, Han K, et al. Evaluation of treatment response in hepatocellular carcinoma in the explanted liver with Liver Imaging Reporting and Data System version 2017. *Eur Radiol* 2020;30:261-271
15. Chaudhry M, McGinty KA, Mervak B, Lerebours R, Li C, Shropshire E, et al. The LI-RADS version 2018 MRI treatment response algorithm: evaluation of ablated hepatocellular carcinoma. *Radiology* 2020;294:320-326
16. Yu JS, Kim YH, Rofsky NM. Dynamic subtraction magnetic resonance imaging of cirrhotic liver: assessment of high signal intensity lesions on nonenhanced T1-weighted images. *J Comput Assist Tomogr* 2005;29:51-58
17. Tirkes T, Mehta P, Aisen AM, Lall C, Akisik F. Comparison of dynamic phase enhancement of hepatocellular carcinoma using gadoxetate disodium vs gadobenate dimeglumine. *J Comput Assist Tomogr* 2015;39:479-482
18. Kim S, Mannelli L, Hajdu CH, Babb JS, Clark TW, Hecht EM, et al. Hepatocellular carcinoma: assessment of response to transarterial chemoembolization with image subtraction. *J Magn Reson Imaging* 2010;31:348-355
19. Gordic S, Corcuera-Solano I, Stueck A, Besa C, Argiriadi P, Guniganti P, et al. Evaluation of HCC response to locoregional therapy: Validation of MRI-based response criteria versus explant pathology. *J Hepatol* 2017;67:1213-1221
20. Kim DH, Choi SH, Byun JH, Kang JH, Lim YS, Lee SJ, et al. Arterial subtraction images of gadoxetate-enhanced MRI improve diagnosis of early-stage hepatocellular carcinoma. *J Hepatol* 2019;71:534-542
21. Sundarakumar DK, Wilson GJ, Osman SF, Zaidi SF, Maki JH. Evaluation of image registration in subtracted 3D dynamic contrast-enhanced MRI of treated hepatocellular carcinoma. *AJR Am J Roentgenol* 2015;204:287-296
22. American College of Radiology. CT/MRI LI-RADS® v2018. Acr.org Web site. <https://www.acr.org/Clinical-Resources/Reporting-and-Data-Systems/LI-RADS/CT-MRI-LI-RADS-v2018>. Accessed November 3, 2020
23. Cools KS, Moon AM, Burke LMB, McGinty KA, Strassle PD, Gerber DA. Validation of the liver imaging reporting and data system treatment response criteria after thermal ablation for hepatocellular carcinoma. *Liver Transpl* 2020;26:203-214
24. Mannelli L, Kim S, Hajdu CH, Babb JS, Clark TW, Taouli B. Assessment of tumor necrosis of hepatocellular carcinoma after chemoembolization: diffusion-weighted and contrast-enhanced MRI with histopathologic correlation of the explanted liver. *AJR Am J Roentgenol* 2009;193:1044-1052
25. Choi SH, Kim SY, Lee SS, Shim JH, Byun JH, Baek S, et al. Subtraction images of gadoxetic acid-enhanced MRI: effect on the diagnostic performance for focal hepatic lesions in patients at risk for hepatocellular carcinoma. *AJR Am J Roentgenol* 2017;209:584-591